ISBN: 978-3-95450-208-0 doi:10.18429/JACoW-IPAC2019-MOPTS081

DESIGN OF THE TRANSFERLINE TO THE ESS TARGET AND BEAM DUMP AT REDUCED BEAM ENERGY

Y.S. Qin[†,1], M. Eshraqi, Y. Levinsen, R. Miyamoto, European Spallation Source ERIC, Lund, Sweden
[1]also at Institute of Modern Physics, Chinese Academy of Sciences (IMP/CAS), Lanzhou, China
and at University of Chinese Academy of Sciences (UCAS), Beijing, China

Abstract

The European Spallation Source (ESS) linac transferlines to the target and beam dump are designed for the 2 GeV beam energy. The commissioning and operation of the accelerator will start at a reduced energy of 571 MeV with the high beta part of the linac unpowered. The beam power at this energy is still above 1 MW and a proper transport from the last accelerating cavity to the target is essential. Beam dynamics design of the High Energy Beam Transport (HEBT) line and Accelerator to Target (A2T) are studied based on this reduced energy in this paper, including phase advance optimization and rematch. Among the factors which are analyzed are the envelope and beam size on the target which are kept close to their values at 2 GeV and losses along the linac and the transferlines.

INTRODUCTION

Figure 1 shows the overview of the ESS linac layout. At a reduced energy of 571 MeV [1, 2, 3], to transport the beam with the power of 1.4 MW to the target stably, no beam loss in the transport line above 1 W/m is tolerated. Thus, the beam envelope needs to be controlled to be stable and phase advance should be smooth. The main work of the paper is focused on beam phase advance smoothing and rematching of each section for the new beam energy. Other problems such as achromaticity, π phase advance in the crossover section [4] and beam size on the target are also studied.

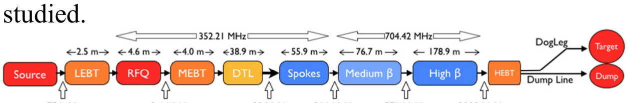

Figure 1: Overview of the ESS linac layout.

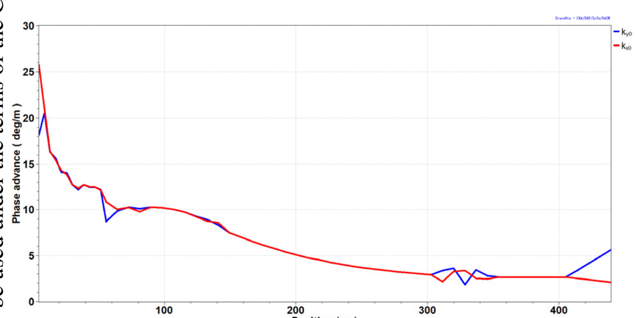

Figure 2: Phase advance per meter from SPK to HEBT for 2 GeV beam.

For 2 GeV beam, the phase advance per meter is smooth along the linac as shown in Fig. 2, except for some periods between different sections because some quadrupoles are adjusted to be matched between adjacent sections (see details in Fig. 11).

For 571 MeV beam, the lattice is rematched from Spoke Linac (SPK) to the target and dump. All simulations presented in this paper were conducted with TraceWin code [5].

REMATCH

Comparing with 2 GeV beam, magnetic rigidity of 571 MeV proton beam decreases from 9.3 T·m to 3.9 T·m, but space charge effect is stronger for the low beam energy. In the High Beta Linac (HBL) section, the rf defocusing disappears with the absence of rf power feeding to the cavities. To keep the beam envelope to be at the same level, the gradient of quadrupoles needs to be adjusted respectively to keep the same phase advance for each period.

HBL

Four quadrupoles near the interface of Medium Beta Linac (MBL) and HBL are used for matching as shown in the red rectangle of Fig. 3. The goal is to keep beam envelope in HBL to be smooth and at the same level as the 2 GeV case, so that beam can be delivered without excessive power loss.

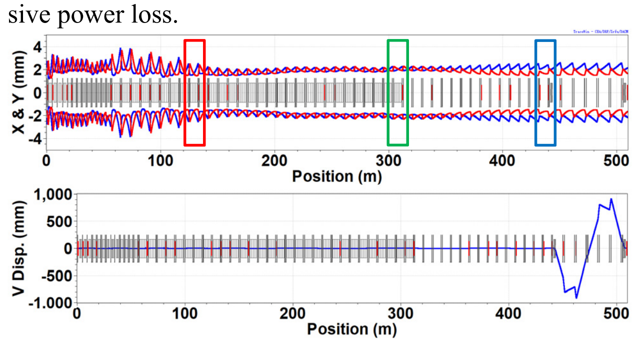

Figure 3: Root Mean Square (RMS) envelope (upper) and the vertical dispersion (lower) from SPK to dogleg for 571 MeV beam (Quadrupoles in the red rectangle are used for matching HBL, green for HEBT, and blue for the dogleg).

HEBT

In the same way done for HBL, four quadrupoles near the interface of HBL and HEBT are adjusted (green rectangle in Fig. 3).

Considering the requirement of phase advance in the dogleg section, beam envelope in A2T section and beam size on the target, the phase advance is optimized and redefined in HEBT section. It decreases in the horizontal plane and increases in the vertical plane smoothly.

† yuanshuai.qin@esss.se

ISBN: 978-3-95450-208-0 doi:10.18429/JACoW-IPAC2019-MOPTS081

The optimized result is shown in Fig. 4. The value of the phase advance in the last period will be discussed in the following two subsections (Eq. (1) and Table 1).

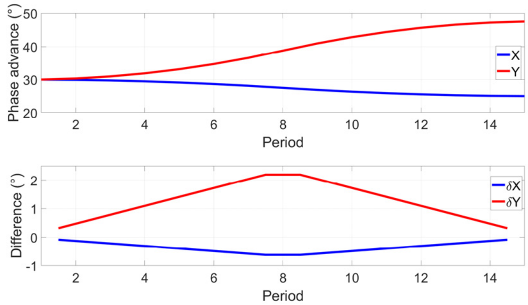

Figure 4: Phase advance transition in the HEBT section for 571 MeV (Upper is phase advance per period, lower is the difference between two adjacent periods).

Dogleg

Six periodic doublets are between the two dipoles and the total phase advance is 360° between the center of the dipoles to make the dogleg achromat [6]. Four quadrupoles in the last two periods of the HEBT section are adjusted as shown in the blue rectangle in Fig. 3.

The length between the center of the two dipoles is 64.50942 m and the periodic length in the HEBT section is 8.52 m, so phase advance in the vertical plane for the last period of HEBT should be

$$360° / 64.50942 \times 8.52 = 47.5465° \quad (1)$$

as shown in Fig. 4.

A2T After Dogleg

There are three doublets in A2T section after the last dipole, where each is referred to as Q_1, Q_2, and etc., as shown in Fig. 5). The requirement of the section is beam waist at Crossover (CO), phase advance requirement between Action Point (AP) and CO, and beam size on the target. Structure phase advance between AP and CO is π and it is adjusted by Q_5-Q_6. After that, Q_1-Q_4 are adjusted for beam waist at crossover and size on the target.

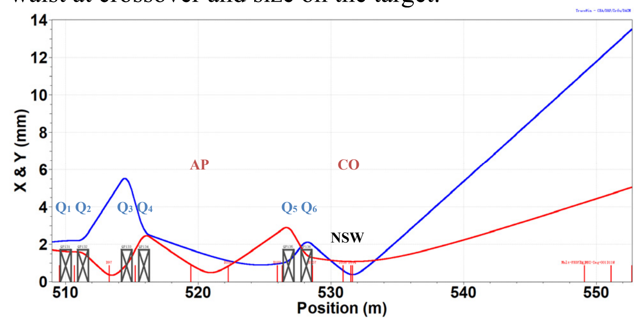

Figure 5: RMS envelope and location of quadrupoles in A2T section after dogleg for 571 MeV beam.

Beam envelope in the horizontal plane at Q_3 is much larger for the 571 MeV case comparing with the 2 GeV case. To avoid beam loss there, phase advance in HEBT and dogleg in the horizontal plane is optimized as shown in Fig. 6. As the horizontal phase advance for the last period of HEBT decreases, beam size on the target gets close to the required value, at the phase advance value of 25°, it gets closest to the desired value with an error of about 0.02%, and is adopted as the optimized value (bold line in Table 1).

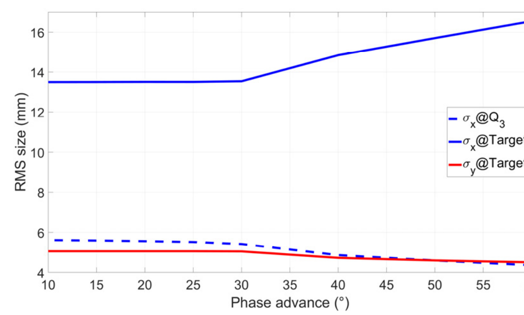

Figure 6: Optimization on phase advance of last period at HEBT.

Table 1: Optimization on the Horizontal Phase Advance for the Last Period of HEBT

Phase advance (°)	σx@Q3 (mm)	σx@Target (mm)	σy@Target (mm)	Required σx @Target (mm)	Required σy @Target (mm)	σx error (%)	σy error (%)
60	4.355	16.549	4.502	13.5	5.05	22.585	-10.851
50	4.595	15.703	4.595	13.5	5.05	16.319	-9.010
40	4.860	14.841	4.723	13.5	5.05	9.933	-6.475
30	5.418	13.537	5.043	13.5	5.05	0.274	-0.139
25	**5.518**	**13.503**	**5.051**	**13.5**	**5.05**	**0.022**	**0.020**
20	5.562	13.505	5.051	13.5	5.05	0.037	0.020
15	5.593	13.498	5.051	13.5	5.05	-0.015	0.020
10	5.615	13.495	5.051	13.5	5.05	-0.037	0.020

There is a long drift from CO to the target. With initial beam parameters of $\{\varepsilon_n, \alpha_0 = 0, \beta_0\}$ at CO, the beta function will be $\beta_t = \beta_0 + \frac{s^2}{\beta_0}$ on the target. For 571 MeV, the same size $\sigma_t = \sqrt{\beta_t \varepsilon_g}$ on the target should be achieved as that in 2 GeV, where $\varepsilon_g = \varepsilon_n/(\beta\gamma)$. It means that beam size at CO would be about 1.4 times larger.

ISBN: 978-3-95450-208-0 doi:10.18429/JACoW-IPAC2019-MOPTS081

Dump Line

The three quadrupoles in the dump line are adjusted manually and beam size on the dump is matched within 0.1% (Table 2).

Table 2: Comparison of Beam Size on the Dump

	RMS_X	RMS_Y
2 GeV	23.085	15.255
571 MeV	23.107	15.242
Difference	0.022 (0.095%)	-0.013 (0.085%)

MULTIPARTICLE SIMULATION

A multiparticle simulation was conducted to check beam loss along the linac and the result shows there is no power loss at Q_3 and CO, even with raster scan [7, 8, 9].

When errors [10, 11, 12] are considered, still no loss was observed at CO, but there is 1 W loss at Q_3 and 52.2 W on the Proton Beam Window (PBW) (Fig. 7).

Figure 7: Beam relative size (the ratio of RMS size and local aperture) and RMS power loss at Q_3 and PBW with errors.

If only raster scan is considered (without errors), beam power loss on the PBW is 2.12 kW. When both considered, it is the same as the case without scan at Q_3 and CO, but power loss on the PBW will increase to 2.87 kW. A possible way for decreasing power loss on the PBW is to decrease beam size on the target. When RMS size on the target is decreased by 10%, power loss on the PBW will be within 1 kW.

COMPARISON

A comparison between the two different energy cases is shown in Figs. 8, 9, 10 and 11, including RMS envelope, emittances, quadrupole gradients and phase advance.

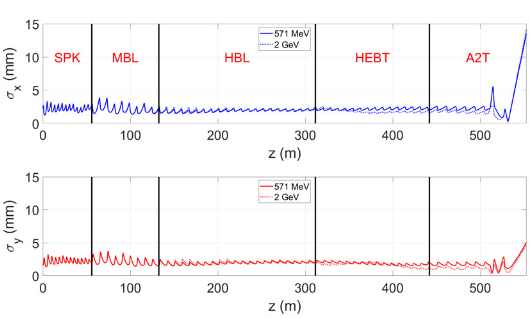

Figure 8: Beam RMS envelope comparison (Beam size at HEBT and A2T sections are larger because lower energy leads to higher geometric emittance).

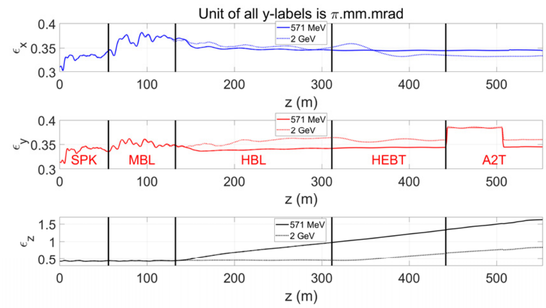

Figure 9: Normalized RMS emittance comparison (The emittance bump in the vertical plane in A2T section is an artifact due to that the dispersion is not taken into account in the emittance calculation).

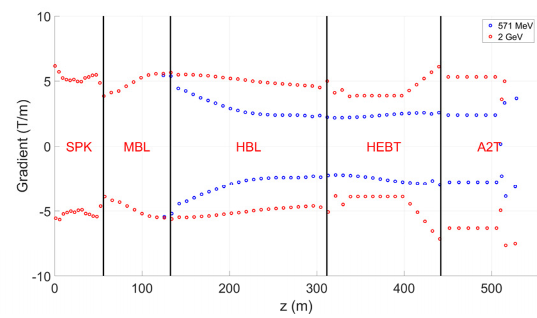

Figure 10: Quadrupole gradients comparison (Gradient of all the quadrupoles is within ±10 T/m and it is lower for the low energy case).

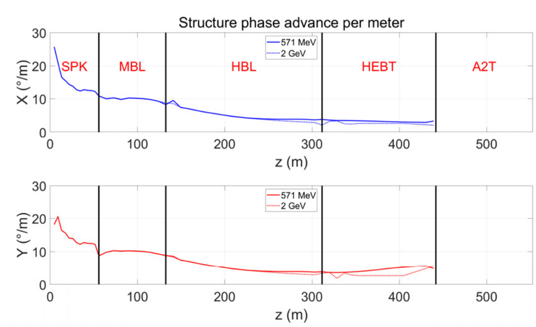

Figure 11: Structure phase advance per meter comparison.

CONCLUSION

To prepare for the initial phase of commissioning when high beta cavities are unpowered, a new lattice for the transport line of 571 MeV beam was designed with Trace-Win. Phase advance in HEBT was optimized to maintain the beam envelope at the same level as the nominal 2 GeV case. Multiparticle simulations with errors and raster scan were conducted and confirmed that no beam loss is present at crossover section and beam loss level at Q_3 and PBW before the target is within the acceptable level.

ISBN: 978-3-95450-208-0 doi:10.18429/JACoW-IPAC2019-MOPTS081

REFERENCES

[1] R. Garoby *et al.*, "The European Spallation Source Design", *Phys. Scr.*, vol. 93, p. 014001, Dec. 2017. doi:10.1088/1402-4896/aa9bff

[2] M. Eshraqi *et al.*, "ESS Linac Beam Physics Design Update", in *Proc. 7th Int. Particle Accelerator Conf. (IPAC'16)*, Busan, Korea, May 2016, pp. 947-950. doi:10.18429/JACoW-IPAC2016-MOPOY045

[3] Y. I. Levinsen *et al.*, "Beam Dynamics of the ESS Linac", in *HB'18*, Daejeon, Korea, Jun. 2018. Pp. 206-209. doi:10.18429/JACoW-HB2018-WEP1WB01

[4] S. Peggs et al., "ESS technical design report", ESS, Lund, Sweden, Tech. Rep. ESS-doc-274-v15, Apr. 2013.

[5] D. Uriot and N. Pichoff, "Status of TraceWin Code", in *Proc. 6th Int. Particle Accelerator Conf. (IPAC'15)*, Richmond, VA, USA, May 2015, pp. 92-94. doi:10.18429/JACoW-IPAC2015-MOPWA008

[6] H. D. Thomsen and S. P. Møller, "The ESS High Energy Beam Transport After the 2013 Design Update", in *Proc. 5th Int. Particle Accelerator Conf. (IPAC'14)*, Dresden, Germany, Jun. 2014, pp. 2121-2123. doi:10.18429/JACoW-IPAC2014-WEPRO073

[7] H. D. Thomsen, A. I. S. Holm, and S. P. Møller, "A Linear Beam Raster System for the European Spallation Source?", in *Proc. 4th Int. Particle Accelerator Conf. (IPAC'13)*, Shanghai, China, May 2013, paper MOPEA005, pp. 70-72.

[8] H. D. Thomsen and S. P. Møller, "The Design of the Fast Raster System for the European Spallation Source", in *Proc. 5th Int. Particle Accelerator Conf. (IPAC'14)*, Dresden, Germany, Jun. 2014, pp. 2118-2120. doi:10.18429/JACoW-IPAC2014-WEPRO072

[9] H. D. Thomsen *et al.*, "The Beam Delivery System of the European Spallation Source", in *HB'16*, Malmö, Sweden, Jul. 2016. pp. 427-432. doi:10.18429/JACoW-HB2016-WEAM7Y01

[10] M. Eshraqi *et al.*, "Statistical Error Studies in the ESS Linac", in *Proc. 5th Int. Particle Accelerator Conf. (IPAC'14)*, Dresden, Germany, Jun. 2014, pp. 3323-3325. doi:10.18429/JACoW-IPAC2014-THPME044

[11] Y. I. Levinsen *et al.*, "Beam Dynamics Challenges in the ESS Linac", in *HB'16*, Malmö, Sweden, Jul. 2016. pp. 315-318. doi:10.18429/JACoW-HB2016-TUAM3Y01

[12] H. D. Thomsen and S. P. Møller, "Performance of the ESS High Energy Beam Transport Under Non-nominal Conditions", in *Proc. 5th Int. Particle Accelerator Conf. (IPAC'14)*, Dresden, Germany, Jun. 2014, pp. 2124-2126. doi:10.18429/JACoW-IPAC2014-WEPRO074